

## **Comparative genomics suggests mechanisms of genetic adaptation toward the catabolism of the phenylurea herbicide linuron in *Variovorax***

**Başak Öztürk, Johannes Werner, Jan P. Meier-Kolthoff, Boyke Bunk, Cathrin Spröer, Dirk Springael**

### **Angaben zur Veröffentlichung / Publication details:**

Öztürk, Başak, Johannes Werner, Jan P. Meier-Kolthoff, Boyke Bunk, Cathrin Spröer, and Dirk Springael. 2020. "Comparative genomics suggests mechanisms of genetic adaptation toward the catabolism of the phenylurea herbicide linuron in *Variovorax*." *Genome Biology and Evolution* 12 (6): 827–41.  
<https://doi.org/10.1093/gbe/evaa085>.

# Comparative Genomics Suggests Mechanisms of Genetic Adaptation toward the Catabolism of the Phenylurea Herbicide Linuron in *Variovorax*

Başak Öztürk<sup>1,2,\*</sup>, Johannes Werner<sup>3</sup>, Jan P. Meier-Kolthoff<sup>4</sup>, Boyke Bunk<sup>4</sup>, Cathrin Spröer<sup>4</sup>, and Dirk Springael<sup>2,\*</sup>

<sup>1</sup>Junior Research Group Microbial Biotechnology, Leibniz Institute DSMZ, German Collection of Microorganisms and Cell Cultures, Braunschweig, Germany

<sup>2</sup>Division of Soil and Water Management, KU Leuven, Belgium

<sup>3</sup>Department of Biological Oceanography, Leibniz Institute for Baltic Sea Research, Rostock, Germany

<sup>4</sup>Department Bioinformatics and Databases, Leibniz Institute DSMZ, German Collection of Microorganisms and Cell Cultures, Braunschweig, Germany

\*Corresponding authors: E-mails: basak.oeztuerk@dsMZ.de; dirk.springael@kuleuven.be.

Accepted: April 20, 2020

**Data deposition:** The genome and plasmid nucleotide sequences have been deposited at EMBL/ENA under the accessions LR594659–LR594661 (PBL-H6), LR594662–LR594665 (RA8), LR594666–LR594670 (SRS16), LR594671–LR594674 (PBL-E5), LR594675–LR594677 (PBS-H4), and LR594689–LR594694 (WDL1).

## Abstract

Biodegradation of the phenylurea herbicide linuron appears a specialization within a specific clade of the *Variovorax* genus. The linuron catabolic ability is likely acquired by horizontal gene transfer but the mechanisms involved are not known. The full-genome sequences of six linuron-degrading *Variovorax* strains isolated from geographically distant locations were analyzed to acquire insight into the mechanisms of genetic adaptation toward linuron metabolism. Whole-genome sequence analysis confirmed the phylogenetic position of the linuron degraders in a separate clade within *Variovorax* and indicated that they unlikely originate from a common ancestral linuron degrader. The linuron degraders differentiated from *Variovorax* strains that do not degrade linuron by the presence of multiple plasmids of 20–839 kb, including plasmids of unknown plasmid groups. The linuron catabolic gene clusters showed 1) high conservation and synteny and 2) strain-dependent distribution among the different plasmids. Most of them were bordered by *IS1071* elements forming composite transposon structures, often in a multimeric array configuration, appointing *IS1071* as a key element in the recruitment of linuron catabolic genes in *Variovorax*. Most of the strains carried at least one (catabolic) broad host range plasmid that might have been a second instrument for catabolic gene acquisition. We conclude that clade 1 *Variovorax* strains, despite their different geographical origin, made use of a limited genetic repertoire regarding both catabolic functions and vehicles to acquire linuron biodegradation.

**Key words:** comparative genomics, plasmid biology, biodegradation, horizontal gene transfer.

## Introduction

Linuron [3-(3,4-dichlorophenyl)-1-methoxy-1-methyl urea] is a phenylurea herbicide that has been widely used for weed control in agriculture. Biodegradation is the major route of linuron dissipation in the environment (Bers et al. 2011). Bacteria belonging to the genus *Variovorax* were isolated from geographically distant locations either as single strains

(Sørensen et al. 2005; Breugelmans et al. 2007; Satsuma 2010) or as members of consortia (Dejonghe et al. 2003; Breugelmans et al. 2007) that have the ability to mineralize and utilize the herbicide for growth. Single strains convert linuron to CO<sub>2</sub> and cell material, whereas in consortia *Variovorax* perform particularly the initial hydrolysis of linuron into the primary metabolite 3,4-dichloroaniline (DCA). The

© The Author(s) 2020. Published by Oxford University Press on behalf of the Society for Molecular Biology and Evolution.

This is an Open Access article distributed under the terms of the Creative Commons Attribution Non-Commercial License (<http://creativecommons.org/licenses/by-nc/4.0/>), which permits non-commercial re-use, distribution, and reproduction in any medium, provided the original work is properly cited. For commercial re-use, please contact journals.permissions@oup.com

metabolic pathway of linuron degradation in *Variovorax* sp. WDL1 and SRS16 are well studied. The linuron hydrolases HylA (identified in WDL1) (Bers et al. 2013) and LibA (identified in SRS16) (Bers et al. 2011) perform the hydrolysis of linuron into DCA and *N,O*-dimethylhydroxylamine (*N,O*-DMHA) (Bers et al. 2011, 2013). In both strains, a multicomponent chloroaniline dioxygenase DcaQTA<sub>1</sub>A<sub>2</sub>B converts DCA to 4,5-dichlorocatechol, whereas chlorocatechol is further metabolized to oxo-adipate by enzymes encoded by the *ccdCFDE* gene cluster (Boon et al. 2001). PCR analysis has shown that other linuron-degrading *Variovorax* share the same catabolic genes. Interestingly, based on 16S rRNA gene phylogeny, the linuron-degrading *Variovorax* strains appear to belong to a clade of *Variovorax* strains that separates from the main bulk of strains including most of the type strains (Breugelmans et al. 2007). The ability to degrade and/or grow on linuron is unique for those strains within the *Variovorax* genus, indicating that they must have genetically adapted by acquiring the catabolic genes by horizontal gene transfer (HGT). This is supported by the observation that in SRS16 and WDL1, the catabolic genes are physically linked with mobile genetic elements (MGE). In SRS16, the DCA catabolic genes are bordered by multiple insertion sequence (IS) elements (Bers et al. 2011). The same applies to *hylA*, the *dca* cluster and the *ccd* cluster in strain WDL1 (Albers, Lood, et al. 2018). Moreover, the three catabolic gene clusters in *Variovorax* sp. WDL1 reside on a large extrachromosomal element that shows several plasmid features including gene functions for conjugation (Albers, Lood, et al. 2018). However, how the genetic composition and context of the catabolic genes and their linkage with MGEs vary between different linuron-degrading *Variovorax* strains and how these relate to the geographic origin of the strains and their phylogeny is yet unknown. Such knowledge will provide insight in the mechanisms that govern the functional evolution of genomes and especially those of organic xenobiotic degraders and more specifically of the genus *Variovorax*. This organism inhabits a wide variety of environments suggesting that it is prone to adaptation to new environmental constraints. To this end, we sequenced the complete genomes of six different linuron-degrading *Variovorax* strains isolated from distantly located geographical areas. We 1) reanalyzed the phylogenetic relationship between the strains and their phylogenetic position within the *Variovorax* genus, 2) examined how their genomes differ with those of *Variovorax* strains that do not degrade linuron, emphasizing on the occurrence and types of MGEs, and 3) compared the structure and surrounding context of the gene clusters involved in linuron metabolism.

## Materials and Methods

### Genome Sequencing, Assembly, and Annotation

The details of the biomass and library preparation for genome sequencing are given in the [supplementary text S1, Supplementary Material](#) online. Genome assembly was performed based on the PacBio reads by means of the RS\_HGAP\_Assembly.3 protocol included in SMRT Portal version 2.3.0 applying target genome sizes of 5 Mb (PBL-E5), 15 Mb (WDL1), and 10 Mb (others). All assemblies showed one chromosomal contig, several extrachromosomal contigs, and several artificial contigs. Artificial contigs were removed from the assembly. The remaining contigs were circularized and assembly redundancies at the ends of the contigs were removed. ORFs on the replicons were ordered using *dnaA* (chromosome) or *repA/parA* (plasmids) as the first ORF. Error correction was performed by mapping the Illumina short reads onto finished genomes using *bwa* v. 0.6.2 in paired-end (sampe) mode using default settings (Li and Durbin 2009) with subsequent variant and consensus calling using VarScan v. 2.3.6 (Parameters: `mpileup2cns --min-coverage 10 --min-reads2 6 --min-avg-qual 20 --min-var-freq 0.8 --min-freq-for-hom 0.75 --P value 0.01 --strand-filter 1 --variants 1 --output-vcf 1`) (Li and Durbin 2009). A consensus concordance of QV60 was reached. Automated genome annotation was performed using Prokka v. 1.8 (Seemann 2014).

### Phylogenomic Analysis of *Variovorax* sp. Plasmids and Genomes

The accession numbers of the genome and plasmid sequences used to construct the phylogenetic trees are listed in [supplementary table S1, Supplementary Material](#) online. First, a phylogenomic analysis of the whole-genome data set was conducted at the nucleotide (nt) level using the truly whole-genome-based Genome-BLAST Distance Phylogeny method (GBDP) (Meier-Kolthoff et al. 2013, 2014; Meier-Kolthoff and Göker 2019). Briefly, GBDP infers accurate intergenomic distances between pairs of genome sequences and subjects resulting distances matrices to a distance-based phylogenetic reconstruction under settings recommended for the comparison of prokaryotic genomes (Meier-Kolthoff et al. 2013). The method is used by both the Genome-to-Genome Distance Calculator 2.1 (Meier-Kolthoff et al. 2013) and the Type Strain Genome Server (Meier-Kolthoff and Göker 2019).

A second phylogenetic analysis based on the plasmids' amino acid sequences was conducted using GBDP as well, except that GBDP distance calculations were done under settings recommended for the analysis of bacteriophage sequences (Meier-Kolthoff and Göker 2017). The reason is that, compared to bacteriophages, the plasmids had similar sequence lengths (Meier-Kolthoff and Göker 2017) and thus promised an equally good performance of the GBDP method when applied to plasmid data. The publicly available plasmid

sequences included in this study were selected based on their relatedness to the newly sequenced plasmids, in order to allocate them into known plasmid groups. In both analyses, a balanced minimum evolution tree was inferred using FastME v2.1.4 with SPR postprocessing each (Lefort et al. 2015). Hundred replicate trees were reconstructed in the same way and branch support was subsequently mapped onto the respective tree (Meier-Kolthoff et al. 2014). For the 16S rRNA gene sequence-based phylogeny, the whole 16S rRNA gene sequences were retrieved from the SILVA database (Quast et al. 2012), and aligned with the SINA aligner (Pruesse et al. 2012). The phylogenies were inferred on the GGDC web server (Meier-Kolthoff et al. 2013) using the DSMZ phylogenomics pipeline (<https://ggdc.dsmz.de/phylogeny-service.php>, last accessed April 05, 2020). The Maximum likelihood (ML) tree was inferred from the alignment with RAxML (Stamatakis 2014). Rapid bootstrapping in conjunction with the autoMRE bootstopping criterion (Pattengale et al. 2010) and subsequent search for the best tree was used. The sequences were checked for a compositional bias using the  $\chi^2$  test as implemented in PAUP\* (Cummings 2014). All phylogenetic trees were visualized with iTOL (Letunic and Bork 2019).

#### Analysis of *Variovorax* sp. Plasmids

The codon usage of chromosomes and plasmids was calculated with CompareM v. 0.0.23 (Parks 2017). Subsequently, Principal Component Analysis (PCA) was conducted and the principle components were hierarchically clustered using the Ward's criterion with FactoMineR v. 1.36 (Le et al. 2008). The replication origins as well as the type IV secretion systems were predicted with oriTfinder v. 1.1 (Li et al. 2018). The relaxase protein sequences were classified into MOB families using MOBScan (Garcillán-Barcia et al. 2009; Garcillan-Barcia et al. 2020). Genes shared between pPBL-E5-2, pSRS16-3, and the chromosomes of the linuron-degrading *Variovorax* were determined with Proteinortho (Lechner et al. 2011). SimpleSynteny (Veltri et al. 2016) was used to determine the positions of the catabolic clusters and associated ORFs, and draw the catabolic cluster illustrations.

## Results and Discussion

### General Genome Features of Linuron-Degrading *Variovorax* Strains

The full-genome sequences of six linuron-degrading *Variovorax* sp. strains, that is, WDL1 (Dejonghe et al. 2003), SRS16 (Sørensen et al. 2005), PBL-H6, PBL-E5, PBS-H4 (Breugelmans et al. 2007), and RA8 (Satsuma 2010) were obtained. Their general genomic features are listed in table 1. Strain WDL1 was recently found to consist of two subpopulations that only deviate in the presence of the *hylA* or *dca* locus (Albers, Lood, et al. 2018). In this study, the genome of

one of these two subpopulations, that is, the one carrying the *hylA* locus was resequenced. The new sequence deviated slightly from the one reported by Albers, Lood, et al. (2018). The 5,400- and 1,240-kbp replicons formed one chromosome of 6.7 Mb, whereas the 1,380-kbp plasmid-like extrachromosomal replicon consisted of two replicons, that is, pWDL1-1 (800 kbp) carrying the linuron catabolic genes and pWDL1-2 (540 kbp).

Chromosome sizes (ranging from 5.99 to 8.36 Mb) and GC content (ranging from 66.24% to 66.86%) of the linuron-degrading *Variovorax* strains were comparable to those of *Variovorax* isolates that do not degrade linuron and for which the genome sequences were available. Sizes of reported nonlinuron-degrading *Variovorax* genomes range between 4.31 and 9.24 Mb (median: 7.2 Mb) with GC contents of 64.6–69.6 (median: 67.4) (supplementary table S1, Supplementary Material online). All linuron-degrading *Variovorax* strains contained a high number of extrachromosomal elements (two to six), including smaller obvious plasmid replicons (20–70 kb) but also larger replicons of >500 kb. The GC content and codon usage of most of those larger extrachromosomal elements substantially differed from those of the chromosome (supplementary fig. S1, Supplementary Material online). They also did not contain any essential genes for cell viability, categorizing them rather as plasmids than as a second chromosome or chromid (Harrison et al. 2010). Replicons pPBL-E5-2 and pSRS16-3, however, showed GC contents and codon usage similar to those of the chromosome, carried plasmid-like replication modules, and shared genes with the chromosomes of other linuron-degrading *Variovorax* strains (67 genes for pSRS16-3, and 65 genes for pPBL-E5-2) classifying them as chromids according to Harrison et al. (2010). In contrast to the genomes of the linuron degraders, none of the genomes of *Variovorax* isolates that do not degrade linuron carried plasmids. IncP-1 plasmids were however reported in three not phylogenetically classified *Variovorax* isolates with unknown genome sequences. Plasmids pHB44 (Zhang et al. 2015) and pBS64 (Zhang et al. 2015) were identified in *Variovorax* strains associated with the mycorrhizal fungus *Laccaria proxima*. They carry genes that increase the *Variovorax* host fitness by enabling metal ion transport and bacitracin resistance (Zhang et al. 2016). Plasmid pDB1 (Kim et al. 2013) in *Variovorax* sp. DB1, carries genes for the biodegradation of the herbicide 2,4-dichlorophenoxyacetic acid (2,4-D). Another feature that distinguished the linuron-degrading strains from the non-degraders is the occurrence of a high number of IS1071 IS elements varying from four to seven copies in the degraders, whereas nondegraders did not carry any IS1071. IS1071 is an IS that was first described bordering the 3-chlorobenzoate catabolic genes of the *Comamonas testosteroni* BRC60 plasmid pBRC60 (Fulthorpe and Wyndham 1992) and was classified as a class II (Tn3-like) transposon (Nakatsu et al. 1991). Since then it has been frequently associated with catabolic

**Table 1**General Properties of the Genome Sequences of Linuron-Degrading *Variovorax* Strains, along with Their Phenotypes and Geographic Origins

Strain	Replicon	Size (kb)	GC%	Number of				Degradation Genes
				ORFs	tRNA Genes	Transposases	IS1071	
WDL1 (linuron to CO <sub>2</sub> ) Belgium	Chromosome	6,724.9	67.2	6,376	56	64		
	pWDL1-1	825.1	62.5	862	44	29	5	<i>hlyA</i> or <i>dca</i> and <i>ccd</i>
	pWDL1-2	565.9	63.5	543	27	24		
	pWDL1-3	207.9	63.7	229		42		
	pWDL1-5	20.1	62.6	25				
	pWDL1-4	25.0	62.6	23		8	1	
	Total	8,368.8		8,058	127	167	6	
PBL-H6 (linuron to CO <sub>2</sub> ) Halen, Belgium	Chromosome	5,990.2	66.8	5,557	54	6		
	pPBL-H6-1	839.2	62.4	883	50	36	5	<i>libA</i> , <i>dca</i> , <i>ccd</i>
	pPBL-H6-2 (PromA)	42.1	63.5	49		1	1	
	Total	6,871.6		6,489		43	6	
PBS-H4 (linuron to DCA) Halen, Belgium	Chromosome	6,429.8	66.9	6,031	57	7		
	pPBS-H4-1	117.4	64.9	95		2		
	pPBS-H4-2 (PromA)	104.9	62.7	112		14	5	<i>hlyA</i> , <i>ccd</i>
	Total	6,652.1		6,238	161	23	7	
RA8 (linuron to DCA) Japan	Chromosome	6,501.6	67.2	6,129	52	7		
	pRA8-1	429.0	64.9	443		8	2	<i>ccd</i>
	pRA8-2	425.3	64.2	419	23	19	2	
	pRA8-3 (IncP-1)	68.4	61.2	63		30	3	<i>libA</i>
	Total	7,424.2		482	23	64	7	
SRS16 (linuron to CO <sub>2</sub> ) Simmelkær, Denmark	Chromosome	5,763.0	67.3	5,469	50	13		
	pSRS16-1	801.4	62.5	852	50	19	2	<i>dca</i> , <i>ccd</i>
	pSRS16-2	560.6	64.5	555		31		
	pSRS16-3	478.8	67	469		0		
	pSRS16-4 (IncP-1)	71.1	61.9	66		12	3	<i>libA</i>
	Total	7,674.9		7,411	100	75	5	
PBL-E5 (linuron to CO <sub>2</sub> ) Simmelkær, Denmark	Chromosome	5,660.8	67.3	5,421	47	10		
	pPBL-E5-1	801.5	62.5	844	50	20	1	<i>dca</i> , <i>ccd</i>
	pPBL-E5-2	553.0	67.1	550		4		
	pPBL-E5-3 (IncP-1)	71.0	61.3	66		11	3	<i>libA</i>
	Total	7,086.4		6,881	97	45	4	

genes in various organisms, primarily  $\beta$ -proteobacteria (Dunon et al. 2018). It often flanks the catabolic genes at both sites, forming a composite transposon structure (Fulthorpe and Wyndham 1992). The element has been suggested to play a primary role in the acquisition and subsequent distribution of adaptive genes and especially catabolic functions in bacteria (Providenti et al. 2006; Dunon et al. 2013, 2018).

#### Phylogenetic Analysis of Linuron-Degrading *Variovorax* Strains

The phylogenetic relatedness between the linuron-degrading *Variovorax* strains was determined by digital DNA:DNA hybridization values (dDDH) (supplementary table S2, Supplementary Material online). With the exception of PBL-E5 and SRS16, which represent the same species (dDDH value of 86%), all linuron-degrading *Variovorax* were

designated as distinct species, and none of them belonged to any type species. Their phylogenetic divergence strongly indicates that the five degraders acquired linuron degradation genes independently as opposed to being derived from one common ancestral linuron degrader. Whole genome-based phylogeny showed that the *Variovorax* species sequenced to date separated into two clades (clade 1 and clade 2), and that the linuron degraders are closely related species, all belonging to clade 1 (fig. 1). The tree topology remained the same when only the linuron degrader chromosomes were used (supplementary fig. S2, Supplementary Material online). This separation largely replicated the 16S rRNA gene sequence-based phylogeny (supplementary fig. S3, Supplementary Material online), with the exception of *Variovorax soli* and *Variovorax* sp. OV329. The low dDDH values of the *V. soli* genome with the degrader genomes (24.7–25.7%) however confirmed that they are distantly related.

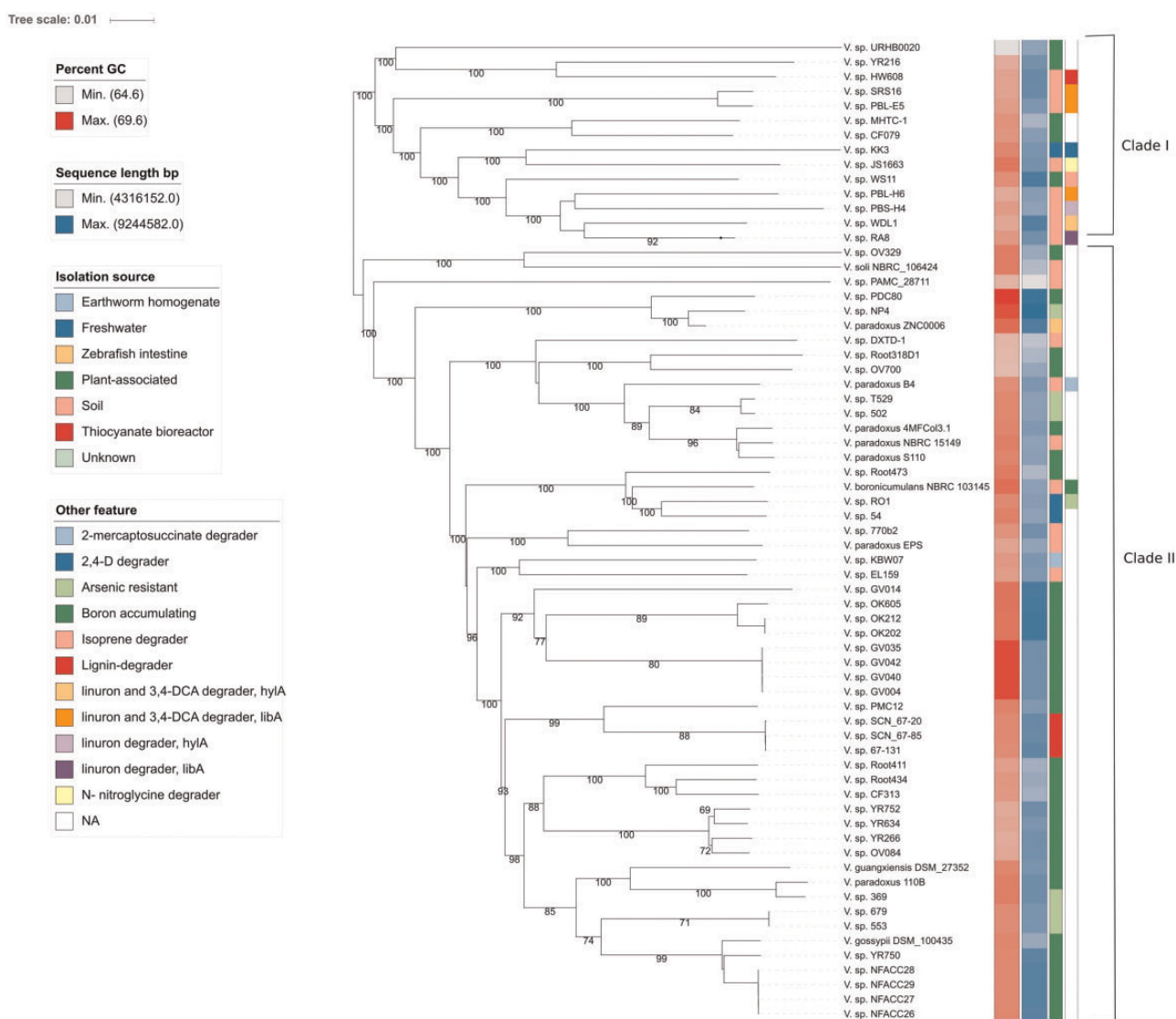


**Fig. 1.**—GBDP phylogenomic analysis of the *Variovorax* whole-genome sequence data set. The branch lengths are scaled in terms of GBDP distance formula  $d_5$ . The numbers above branches are GBDP pseudo-bootstrap support values from 100 replications, with an average branch support of 80.6%. Leaf labels are further annotated by their genomic G + C content, genome sequence length, phenotypic attributes, and origin of isolation. The two *Variovorax* clades are indicated.

In addition to the linuron-degrading *Variovorax* strains, clade 1 included various other isolates but no type species. From those, a closed genome sequence was only available for the lignin-degrading soil isolate strain HW608 (Woo et al. 2017). The phylogenetic position of the linuron-degrading strains was independent of either the geographic origin, the capacity to degrade linuron completely or partially to DCA, or the presence of specific catabolic genes involved in linuron biodegradation. Clade 2 contained the majority of the *Variovorax* strains, including the species *Variovorax boronicumulans*, *V. soli*, *Variovorax paradoxus*, *Variovorax gossypii*, and *Variovorax guangxiensis*. Interestingly, in contrast to the clade 2 strains, nonlinuron-degrading strains from clade 1 were

often associated with the catabolism of natural and anthropogenic organic compounds such as *Variovorax* sp. WS11 (an isoprene-degrading phyllosphere isolate; Crombie et al. 2018), KK3 (a 2,4-D-degrading freshwater isolate; Wang et al. 2017), and JJ 1663 (an *N*-nitroglycine-degrading activated sludge isolate; Mahan et al. 2017). As such, including the linuron degraders, eight of the 14 clade 1 strains were degraders of anthropogenic compounds. Clade 2, however, included only one xenobiotic-degrading isolate (one in 55 strains), that is, *V. boronicumulans* J1 (Satola et al. 2013) that degrades the neonicotinoid thiacloprid but only cometabolically (Zhang et al. 2012). These results indicate that the linuron-degrading strains belong to a *Variovorax* clade or

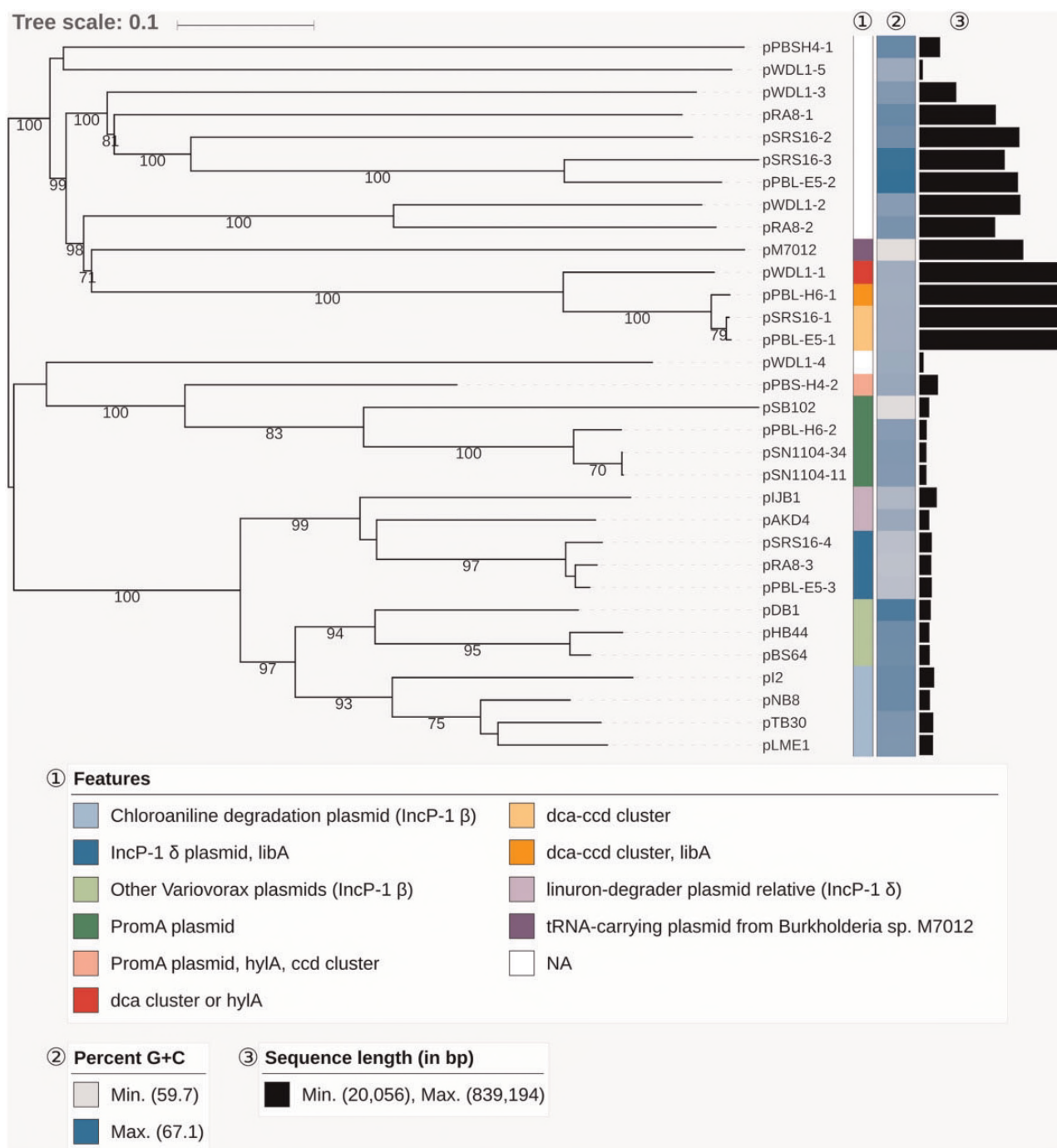


**Fig. 2.**—GBDP phylogenomic analysis of *Variovorax* plasmids and relevant relatives. The branch lengths are scaled in terms of GBDP distance formula  $d_6$ . The numbers above branches are GBDP pseudo-bootstrap support values from 100 replications, with an average branch support of 91.3%. Leaf labels are further annotated by their genomic G + C content, length as well as special attributes. NCBI accession numbers of previously reported plasmid sequences: pM7012 (NC\_022995.1), pSB102 (AJ304453.1), pSN1104-34 (AP018708.1), pSN1104-11 (AP018707.1), pJb1 (JX847411.1), pAKD4 (GQ983559.1), pDB1 (JQ436721.1), pHB44 (KU356988.1), pBS64 (KU356987.1), pl2 (JF274989.1), pNB8 (NC\_019264.1), pLME1 (NC\_019263.1), and pTB30 (NC\_016968.1).

originates from a common ancestor that is/was more prone to genetic adaptation and hence specialization toward the biodegradation of anthropogenic compounds. The clade

separation of strains with and without biodegradation capacity has not been observed before in other genera (Tabata et al. 2016; Kim et al. 2018).

**Table 2**

Overview of Plasmid Replication and Conjugation Systems Identified in Linuron-Degrading *Variovorax* Strains

Plasmid	Relaxase	T4CP	T4SS	<i>oriT</i>	Rep/Par Module
pPBL-E5-1	n.f.	34% YP_001911165	TraALBFHJDNUW, TrbC, VirB4	n.f.	RepB-ParAB
pWDL1-1					
pSRS16-1					
pPBL-H6-1					
pSRS16-2	TraI 49% YP_195891 (MOB <sub>p</sub> )	72% NP_990928.1	TrbLJIHGFEDCB, TraJ, VirB1	P	RepB-ParAB
pSRS16-3 (chromid)	n.f.	n.f.	n.f.	n.f.	RepB-ParAB
pPBL-E5-2 (chromid)					
pSRS16-4	TraI 100% YP_006965894.1 (MOB <sub>p</sub> )	100% NP_990928.1	TrbBCDEFGHIJKLN, TraXF	P	RepB-ParAB
pRA8-2					
pPBL-E5-3					
pPBL-H6-2	TraS 79% CAC79161 (MOB <sub>p</sub> )	67% YP_001672044	VirB123456891011, VirD4	P	RepA
pPBS-H4-2					
pRA8-1	Rel 81% SDZ72275.1 (MOB <sub>p</sub> )	45% WP_010895213	VirB23456891011, VirD4	n.f.	RepB-ParAB
pRA8-2	n.f.	n.f.	n.f.	n.f.	RepB-ParAB
pPBS-H4-1	TraA 37% AAV52093 (MOB <sub>p</sub> )	n.f.	n.f.	n.f.	RepA
pWDL1-2	n.f.	n.f.	n.f.	n.f.	RepB-ParAB
pWDL1-3	Rel 84% WP_093180082.1 (MOB <sub>p</sub> )	45% WP_010895213	VirB23456891011, VirD4, TrbB	n.f.	RepAB
pWDL1-4	n.f.	n.f.	n.f.	n.f.	ParAB
pWDL1-5	n.f.	38% AEY63616	VirB568, TraD	n.f.	RepA
chrWDL1			TrbBCDEJLFGI, VirD4, TraF		
chrSRS16			TrbBCDEJLFGI, VirD4		
chrRA8			n.f.		
chrPBL-H6			TrbBCDEJLFGI, VirD4		
chrPBL-E5			TrbBCDEJLFGI, VirD4		
chrPBS-H4			TrbBCDEJLFGI, VirD4		

NOTE.—For the relaxase and T4SS, the % identity on amino acid level to the nearest relative as well as the accession number are given. The plasmids were classified into MOB classes if applicable. T4SS, type IV secretion system; T4CP, type IV coupling protein; n.f., not found; P, present.

### Plasmids Hosted by Linuron-Degrading *Variovorax* sp

Phylogenetic analysis of the entire plasmid sequences clustered the plasmids identified in the linuron-degrading *Variovorax* sp. strains, into both known and novel plasmid groups (fig. 2). Some of the plasmids occur in multiple strains in which they are highly conserved (supplementary fig. S2, Supplementary Material online). Table 2 shows an overview of the replication and conjugation systems encoded on these plasmids. Twelve plasmids have type IV secretion system genes (T4SS) which facilitate conjugative transfer, but the origin of transfer (*oriT*) could not always be determined.

### Known Conjugative Plasmids and Their Role in Linuron Degradation in Linuron-Degrading *Variovorax* Strains

Plasmids pPBL-E5-3, pRA8-3, and pSRS16-4 were classified as IncP-1 $\delta$  plasmids. The three plasmids were 99% identical at the nt level over the entire plasmid sequence and carry the *libA* locus between *trfA* and *oriV*, a known insertion hot spot for accessory genes in IncP-1 plasmids (Dunon et al. 2018). Catabolic IncP-1 $\delta$  plasmids have been reported before either isolated by means of exogenous isolation (Sen et al. 2010) or from isolates (Xia et al. 1998). They all carry 2,4-D catabolic genes between *trfA* and *oriV*. The above-mentioned

*Variovorax* plasmids pDB1 (Kim et al. 2013), pHB44 (Zhang et al. 2015), and pBS64 (Zhang et al. 2015) are also IncP-1 plasmids but belong to the IncP-1  $\beta$  group.

Instead of IncP-1 plasmids, PBL-H6 and PBS-H4 carried PromA plasmids. PromA plasmids form a group of self-transmissible broad host range plasmids. Plasmid pPBS-H4-2 carries *hlyA* and the *ccd* gene cluster each of them bordered at both ends by an IS1071 element, whereas pPBL-H6-2 carries an isolated IS1071 element. In addition, between the *hlyA* and *ccd* loci, the accessory gene region of pPBS-H4-2 carries genes related to plasmid replication and maintenance such as *repAB* and *parAB* and a fifth IS1071. These extra *parAB* genes are unrelated to the pPBS-H4-2 backbone *parAB* genes. Plasmids pPBL-H6-2 and pPBS-H4-2 are most closely related to the PromA  $\gamma$  plasmids pSN1104-11 and pSN1104-34 (Yanagiya et al. 2018) that were isolated by exogenous isolation and hence represent the first PromA  $\gamma$  plasmids obtained from isolates. Their presence in *Variovorax* extends the host range of PromA  $\gamma$  plasmids, as is the case for PromA  $\alpha$  and PromA  $\beta$  plasmids, to  $\beta$ -proteobacteria. Plasmid pPBS-H4-2 is the first catabolic PromA plasmid, and is one of the few non-cryptic PromA plasmids (Mela et al. 2008). The often cryptic character of PromA plasmids has been the subject of a debate because it might harness their stability as they do not benefit

the host fitness. It was suggested that they mainly support the conjugative transfer of other mobilizable replicons (Mela et al. 2008). The finding that PromA plasmids carry catabolic genes shows that they, as is the case for IncP-1 plasmids, can indeed acquire and distribute genes beneficial for the host. The location of cargo genes in both pPBS-H4-2 and pPBL-H6-2 (near *virD2*) differs from this in other PromA plasmids (near *parA*) (Van der Auwera et al. 2009) and identifies the *virD* locus as an alternative hot spot for insertion of accessory genes in PromA plasmids.

### Novel Putatively Conjugative Plasmids in Linuron-Degrading *Variovorax* Strains

Other plasmids than IncP1 and PromA plasmids were identified that carry homologs of TS44 genes (table 2), that is, pWDL1-3 and pWDL1-5, pRA8-1 and pSRS16-2. None of those plasmids categorized into a known plasmid incompatibility group. Although they carry T4SS genes, the origin of transfer (*oriT*) and the gene encoding for the type IV coupling protein (T4CP) could not always be identified. The relaxase, which is required for conjugative transfer (Smillie et al. 2010), could only be identified in pWDL1-3 and was assigned to the MOB<sub>p</sub> family (Garcillán-Barcia et al. 2009). Plasmid pWDL1-3 carries a remarkably high number of 41 putative ISs but no *IS1071*, and several gene clusters for xenobiotic degradation. Among these is a gene cluster that encodes for homologs (40–43% amino acid identity) of proteins encoded by the *tphA1A2A3BR*-gene cluster for terephthalate degradation in *Comamonas* sp. E6 (Sasoh et al. 2006) as well as of benzoate 1,2-dioxygenase subunits. pRA8-1 is distantly related to pWDL1-3 and carries the *ccdCFBD* operon. In addition, it contains homologs of genes encoding for the biodegradation of nonchlorinated catechols, as well as for cation efflux proteins CusABF (Franke et al. 2003) and the cadmium transport protein CadA (Tsai et al. 1992), flanked by *IS1071*. The small pWDL1-5 carries no cargo genes. A highly similar plasmid (99% nt identity, 72% coverage), also without cargo, is present in the chlorobenzene-degrading *Pandoraea pnomenusa* strain MCB032 (Baptista et al. 2008). The finding of this plasmid group in two different genera/families of the same bacterial order indicates its transferability within *Burkholderiales*. The Trb homologs encoded by pSRS16-2 as well as the *oriT* are highly similar (75–80%) to those encoded by IncP-1 plasmids. However, unlike IncP-1 plasmids, pSRS16-2 does not carry *trfA*, and its size (560 kb) is much larger than IncP-1 plasmids. Plasmid pSRS16-2 encodes for a broad range of functions, including 37 transport-related proteins, 18 proteins related to aromatic degradation, and 31 ISs (but without *IS1071*). We conclude that this plasmid represents a novel plasmid group, with conjugative transfer machinery similar to that of IncP-1 plasmids.

### Chromids pSRS16-3 and pPBL-E5-2

The closely related replicons pPBL-E5-2 and pSRS16-3 carrying the *repB-parAB* replication-partitioning module do not contain homologs of genes related to conjugal transfer, suggesting that they are not self-transmissible. Both replicons carry distantly related homologs of catabolic genes such as *tfdA* encoding conversion of 2,4-D (33% amino acid identity) in *Cupriavidus necator* JMP134 (Plumeier et al. 2002), and the *dmpKLMNOPQBCDEFGHI* gene cluster for phenol degradation (45–66% amino acid identity) in *Pseudomonas* sp. CF600 (Shingler et al. 1992), as well as the *phnCDEGHJKLMN* gene cluster for phosphonate uptake and degradation (45–62% amino acid identity) in *Escherichia coli* K12 (Jiang et al. 1995).

### tRNA-Carrying Megaplasmids in Linuron-Degrading *Variovorax* sp

Pairwise alignment showed that pPBL-H6-1, pSRS16-1, pPBL-E5-1, and pWDL1-1 are highly identical to one another. They show 99% nt identity over the entire aligned sequence length including the putative replication/partitioning module *repB-parAB* (Supplementary fig. S4, Supplementary Material online). Plasmid pPBL-H6-1 carries all three gene clusters required to convert linuron to 3-oxoadipate, whereas pSRS16-1 and pPBL-E5-1 only carry *dcaQTA1A2BR* and *ccdCFDE*. The pWDL1-1 variant sequenced in this study carries the *ccdCFDE* genes and the *hlyA* gene. The proteins encoded by the *repB-parAB* module show only slight similarity to their nearest relatives (27%, 48%, and 39% amino acid similarity for RepB, ParA, and ParB, respectively) and hence the four mega-plasmids might represent a new plasmid group, potentially specific for *Variovorax*. All four plasmids carry *traALBFHJDNUNWG* and *trbCG* homologs, suggesting that they might be transferrable. They however have low identity at amino acid level (30–43%) to the nearest relatives involved in conjugative transfer. No putative relaxase was found.

Strikingly, the four megaplasmids carry tRNA genes that encode for all the proteinogenic amino acid codons. Unlike the scattered appearance of the tRNA genes located on the chromosome, the plasmid-encoded tRNA genes are concentrated in one array. Except for the tRNA encoding for codons glutamine (CAG) and arginine (CGC), all tRNAs on these plasmids are also present on the chromosome. In all four hosts, these two codons are preferred by both plasmids and the chromosome, however, multiple other tRNAs encode for these amino acids on the chromosome, suggesting that although the plasmid-encoded tRNAs may enhance gene expression, they are not essential for expression of plasmid genes. pSRS16-1 further lacks the tRNA for valine (CAC), which is preferred by both the chromosome and plasmids; however, this tRNA is present in pSRS16-2 as well as in the chromosome.

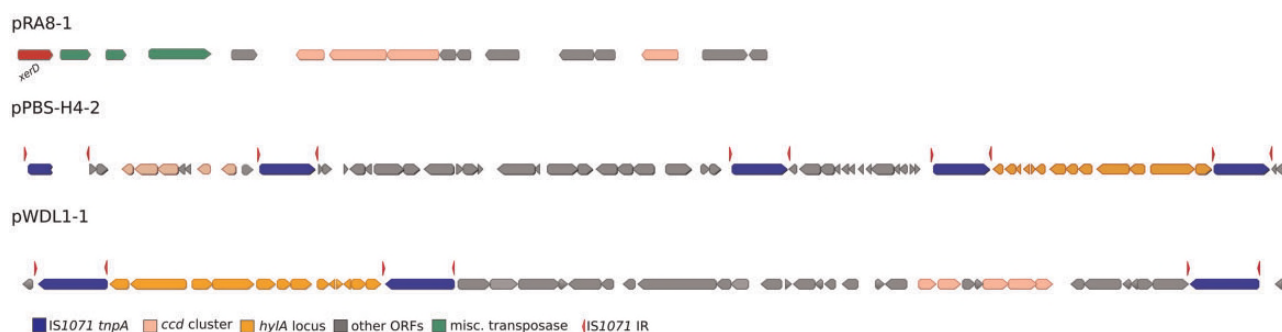


**Fig. 3.**—Genomic context of linuron-catabolic genes in strains WDL1, RA8, and PBS-H4. The *hylA* and *ccd* loci on the plasmids pPBS-H4-2, pWDL1-1, and pRA8-1, as well as flanking genes are illustrated. Broken arrows indicate ORFs which were truncated by immature stop codons, due to point mutations. IS1071 inverted repeats (IR) are indicated by the red arrow points. Non-catabolic ORFs as well as hypothetical genes are indicated in gray.

Other plasmids that carry tRNA genes in the linuron-degrading strains are pRA8-2 and pWDL1-2. These plasmids are distantly related to pPBL-H6-1, pSRS16-1, pPBL-E5-1, and pWDL1-1 and also carry the tRNA genes in an array. However, their tRNAs do not encode for all proteinogenic amino acids and are all redundant. The two plasmids neither have functions for conjugal transfer nor carry catabolic genes but encode for putative heavy metal resistance, like the cobalt–zinc–cadmium efflux system encoded by *czcABCD* (Rensing et al. 1997; Legatzki et al. 2003), the copper-response two-component system encoded by *cusRS* and *cusABRS* (Franke et al. 2003), and mercury resistance encoded by *merACPTR* (Barkay et al. 2003). Unlike pWDL1-2, pRA8-2 carries an IS1071 adjacent to a gene cluster encoding for homologs of the toxin–antitoxin system proteins DinJ–YafQ (Armalyte et al. 2012) and the antirestriction protein KlcA that plays a role in evading host restriction systems during conjugative transfer (Serfiotis-Mitsa et al. 2010).

The presence of tRNA genes on large plasmids has been reported before in other bacteria (Puerto-Galan and Vioque 2012; Sakai et al. 2014; Bottacini et al. 2015; Morgado and Vicente 2018). None of these plasmids however related to the tRNA-carrying *Variovorax* plasmids. In *Bifidobacterium breve*, the tRNA-encoding plasmid improves gene expression from both the chromosome and the plasmid (Bottacini et al. 2015), whereas in *Anabaena* sp. PCC 7120, it is dispensable for growth (Puerto-Galan and Vioque 2012). Other MGEs different from plasmids (Alamos et al. 2018) as well as bacteriophages (Pope et al. 2014), encode for tRNA genes. In the acidophilic, bioleaching bacterium *Acidithiobacillus ferrooxidans*, the tRNA genes are located on an integrative conjugative element and are likely not essential for growth (Alamos et al. 2018).

Another feature that sets plasmids pPBL-H6-1, pPBL-E5-1, pSRS16-1, and pWDL1-1 apart is the presence of a CRISPR3-Cas cassette, which is identical in all of them. The cassette consists of a CRISPR array with 15 spacers, in addition to the genes encoding for a Cas6/Cse3/CasE-type endonuclease, the Cascade subunits CasA, CasB, CasC, and CasD and the

CRISPR-associated proteins Cas1 and Cas2, which is similar to the class I-E CRISPR-Cas systems (Koonin et al. 2017). The CRISPR-defense system protects bacteria and archaea against MGEs and phages (Pothier et al. 2011), and can be transferred horizontally (Godde and Bickerton 2006; Bottacini et al. 2015). Although the exact direct repeats (DRs) of the CRISPR structure were also found in the *Serpentinomonas mccroryi* strain B1 genome (GCA\_000828915.1), the spacer sequences did not have any match in the CRISPR databases. Interestingly, no CRISPRs were found in other *Variovorax* genomes available in public databases, with the exception of *Variovorax* sp. PDC80 (GCF\_900115375.1), which carries a class I-F CRISPR-Cas system with spacers unrelated to those of the megaplasmids.

### Genomic Context of the Linuron-Catabolic Loci in the Linuron-Degrading *Variovorax* Strains

We analyzed the presence, location, and genomic context of *hylA* and *libA* genes for linuron hydrolysis, *dcaQTA1A2BR* genes for DCA conversion to 4,5-chlorocatechol (Król et al. 2012) and *ccdCDEF* genes for 4,5-dichlorocatechol degradation (Bers et al. 2011, 2013) in each of the degraders genome. These genes were not present in any of the other publicly available *Variovorax* genomes.

### Genomic Context of the Linuron-Hydrolysis Genes *hylA* and *libA*

The linuron hydrolysis genes *hylA* and *libA* were highly conserved among the different strains. The six linuron degraders carried either *hylA* or *libA*, but never both. *hylA* is present in one copy in strains PBS-H4 and WDL1. As in WDL1 (Albers, Lood, et al. 2018), *hylA* in PBS-H4 makes part of a larger gene cluster of 13 ORFs that is highly conserved among the two *hylA* hosting strains (99–100% nt identity and complete synteny). In both strains, the gene cluster is flanked at both sites by IS1071 composing a composite transposon structure (fig. 3). The functions of the *hylA* associated ORFs, and in particular the downstream ORFs, are currently unclear, but

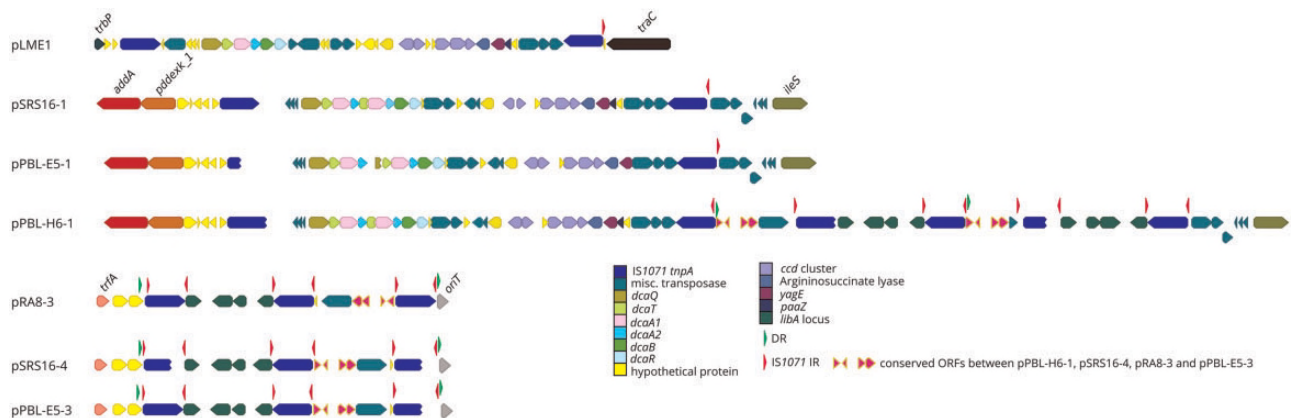


**Fig. 4.**—Genomic context of linuron-catabolic genes in strains SRS16, PBL-H6, RA-8, and PBL-E5. On the upper panel, the *dca* and *ccd* clusters on plasmids pPBL-E5-1, pSRS16-1, and pPBL-H6-1 as well as the *Delftia acidovorans* plasmid pLME1 are illustrated, together with flanking genes and genes directly neighboring each IS1071 element. In the lower panel, the *libA* gene-associated IS1071 elements are illustrated for pPBL-H6-1, pPBL-E5-3, pSRS16-4, and pRA8-3. The backbone genes flanking the IS1071 insertion sites are annotated on the figure. IS1071 IRs and DRs are indicated by red and green arrow points, respectively. Broken arrows indicate ORFs which were truncated by immature stop codons, caused by point mutations.

their conservative nature indicates that they play a role in linuron hydrolysis. Albers, Weytjens, et al. (2018) showed the transcriptional upregulation of the downstream *luxR* homologs when WDL1 is degrading linuron within a consortium. The *hylA*-carrying composite transposon likely originated by inserting the *hylA* gene together with its downstream ORFs in a precursor composite transposon carrying the *iorAB* and *dca* gene clusters as suggested by the presence of *iorAB* and a *dcaQ* remnant directly upstream of *hylA*. Interestingly, the *dcaQ* gene that directly flanks *hylA*, is truncated at a different nt residue in WDL1 and in PBS-H4 (in PBS-H4 at nt position 749, in WDL1 at nt position 689), which suggests that the *hylA* gene and its associated downstream ORFs were independently acquired by the composite transposons present in the two strains. We identified exact copies of both the WDL1 and the PBS-H4 *hylA*-carrying composite transposon, that is, with identical *hylA*-*dcaQ* junctions in a linuron-degrading *Hydrogenophaga* isolate as well as in an exogenously isolated plasmid indicating that WDL1 and PBS-H4 recruited the *hylA* locus through an already existing composite transposon structure (Werner et al. 2020). However, no direct indication was found of the mobile character of the structure as no direct repeats (DRs) could be recognized bordering the outward inverted repeat (IR) of the flanking IS1071 ISs.

The *libA* gene is present in SRS16, PBL-E5, RA8, and PBL-H6. In SRS16, PBL-E5 and RA8, *libA* is carried by an IncP-1 plasmid (pSRS16-4, pPBL-E5-3, and pRA8-3, respectively), whereas in PBL-H6 it is carried as two copies by the tRNA-carrying megaplasmid pPBL-H6-1. In all four strains, *libA* makes part of a larger highly conserved gene cluster of four ORFs flanked at both borders by IS1071. This four-ORF gene cluster contains a *luxR*-family transcription regulator directly adjacent to *libA* followed by an IS91-family IS. As such, as for

the *hylA* locus, the *libA* locus is encompassed in a composite transposon structure (fig. 4). However, the two IS1071 elements are in indirect orientation hampering theoretically the mobility of the composite transposon structure as a discrete unit. Interestingly, in all four strains, directly adjacent to the *libA* containing composite transposon structure, a strongly conserved gene cluster was found bordered by a third IS1071 in direct orientation with the first IS1071. DRs can be found at the outward border of the first IS1071 and of the third IS1071, indicating that the *libA* locus is indeed mobile but that this mobility relates to a super composite transposon encompassing all three IS1071 elements and intermediate DNA. Within this super composite transposon, some of the *tnpA* genes appear truncated and hence not functional but IRs are always present at the outer borders and the transposon structure contains at least one complete and hence functional *tnpA*. As suggested above for the recruitment of the *hylA* locus, the remarkable conservation of the *libA* locus including its integration into a (super) composite transposon, might suggest that the different *Variovorax* strains recruited the *libA* locus rather through an already existing composite transposon structure carrying the *libA* locus then via independent recruitment events. Strains SRS16 and PBL-E5 were isolated from the same agricultural field, albeit at different times, and hence the IncP-1 plasmid carrying *libA* seems to contribute to the distribution of the *libA* locus in that field. RA8, though, was isolated in Japan, indicating that similar plasmids evolved at different locations, or that the BHR plasmid was transferred across a large geographic distance. In contrast, in PBL-H6, which originated from a Belgian agricultural field, the super composite transposon is found integrated in a replicon different from IncP-1 plasmids, that is, megaplasmid pPBL-H6-1. The plasmid contains two copies of that super composite transposon that share an outer IS1071.

Likely, the second copy is due to duplication of the *IS1071* flanked structure which would lead to the formation of tandem arrays (fig. 4) of the same DNA fragment interspersed with directly oriented copies of *IS1071* (Harmer et al. 2014; Hudson et al. 2014; He et al. 2015). Interestingly, PBL-H6 harbors the cryptic BHR PromA plasmid pPBL6-H-2 carrying a single copy of *IS1071*. Plasmid pPBL6-H-2 might have been implicated in initial recruitment of the *IS1071* associated linuron catabolic genes in PBLH-6 (see discussion below).

### The *dca* and *ccd* Clusters of Linuron-Degrading *Variovorax* Strains

Similar to the *hyla* and *libA* genes, MGEs determine the genomic context of the *dca* and *ccd* genes. PBL-E5, PBL-H6, and SRS16 carry the entire *dca* and *ccd* clusters, which is consistent with their ability to degrade linuron and DCA. The *ccd* clusters of strains PBL-E5, PBL-H6, and SRS16 are on the 800-Mb megaplasmids, directly downstream of the *dca* clusters (fig. 4). In all strains, the entire *dca/ccd* gene cluster is bordered by *IS1071* at both sides. However, the two elements lack the inward-directed IRs and one even lacks additionally the outward-directed IR. Moreover, the outer *IS1071* elements are indirectly oriented. A similar composite transposon configuration including the *dca* and *ccd* genes is found in the chloroaniline degrader *Delftia acidovorans* LME1 (Boon et al. 2001) (fig. 4), except that PBL-H6 and SRS16 have two copies of the *dcaA1A2* genes and PBL-E5 two adjacent copies of the *dcaQTA1A2B* genes with one intact and one truncated *dcaB*. Other chloroaniline degraders like *C. testosteroni* WDL7 and *D. acidovorans* B8c (Król et al. 2012) carry a similar structure but lack the *dcaA1A2* duplications as well as the *ccd* genes (fig. 4). Amino acid-level similarity of the proteins encoded by *dcaQTA1A1BR* and *ccdCFDE* between the three *Variovorax* strains and LME1/WDL7/B8c is ~99% (supplementary table S3, Supplementary Material online). As for the *hyla* and *libA* loci, we hypothesize that the *dca/ccd* gene clusters were obtained by being already integrated into an ancestral composite transposon but that afterwards gene rearrangements occurred that explain the observed variations. This is further supported by the observation that in the chloroaniline-degrading *Comamonas/Delftia* strains, the composite transposon structures carrying *dca/ccd* genes are located on IncP-1 plasmids, whereas in the three *Variovorax* strains they are located on the 800-kb tRNA-carrying megaplasmids. On the other hand, no DRs were detected bordering the *dca/ccd*-carrying composite transposon structure and there is no evidence for transposition. In case of PBL-H6, the *dca/ccd* cluster is directly adjacent to the composite transposon structure carrying *libA* (see above) sharing the outer *IS1071*, hence forming an array of multiple adjacent putative composite transposons that share a single *IS1071* located between them. In all three plasmids, the location of the *dca/ccd* containing composite transposon is the same, marking the corresponding location

as a likely accessory gene insertion hot spot in the megaplasmid.

The *dca* cluster and associated ORFs present on pWDL1-1 are also bordered by two *IS1071* elements, but the composite transposon does not contain a *ccd* cluster and the *dca* genes are rather related (99% nt identity) to the *tadQTA1A2B* encoding for conversion of aniline to catechol in *Delftia tsurhatensis* AD9 (Liang et al. 2005). The *ccd* cluster, present on pWDL1-1, also differs substantially from those of PBL-E5, PBL-H6, and SRS16 and overall the genes are relatively distantly related to other known chlorocatechol degradation genes (supplementary table S3, Supplementary Material online). This cluster is located in the vicinity of either *hyla* or the *dca* genes, depending on the WDL1 subpopulation (Albers, Lood, et al. 2018). WDL1-1 *hyla/dca* clusters and *ccd* cluster are separated by a stretch of DNA of ~20 kb containing 19 ORFs, forming as such another array of putative composite transposons sharing *IS1071* (fig. 3). Further downstream of the *ccd* cluster another *IS1071* is located.

The *ccd* gene clusters in the non-DCA degraders PBS-H4 and RA8 are identical to those of WDL1. In PBS-H4, the *ccd* cluster is on the PromA plasmid pPBS-H4-2, that also bears the *hyla*-carrying composite transposon. The *ccd* cluster is flanked by *IS1071* at both sites and separates from the *hyla* locus by a stretch of ~32 kb of DNA containing 35 noncatabolic ORFs as well as a another *IS1071*. As such, the cargo on pPBS-H4-2 forms another multimeric array of putative composite transposons sharing *IS1071* (fig. 3). Interestingly, the noncatabolic ORFs carries the aforementioned genes related to plasmid replication and maintenance, as well as 13 hypothetical genes. No DR could be detected in this super composite transposon structure. In RA8, the *ccd* cluster is located on pRA8-1. This cluster is flanked by multiple IS elements but unrelated to *IS1071* genes and hence is the only linuron-catabolic gene cluster without neighboring *IS1071* in the linuron-degrading *Variovorax* strains (fig. 3).

Overall, the analysis of the genetic context of the genes involved in linuron catabolism, either upstream or downstream functions in the pathway, indicates that *IS1071* played an essential role in the plasmidic acquisition of the catabolic genes and genetic adaptation of *Variovorax* toward the ability to degrade linuron. The phenomenon that *IS1071* elements are associated with genes involved in xenobiotic degradation was previously reported using both cultivation-dependent (Boon et al. 2001; Martinez et al. 2001; Sota et al. 2003; Sen et al. 2010) and cultivation-independent (Dunon et al. 2018) methods. Subsequent inter- and intramolecular transposition of *IS1071* is thought to lead to the assembly of catabolic genes into a composite transposon structure with the recruited genes flanked by *IS1071* at both sites (Nakatsu et al. 1991; Di Gioia et al. 1998). The new composite transposon structure might then move as a discrete unit between different replicons (Casacuberta and González 2013) although this has never been shown for composite transposons flanked by

*IS1071*. However, transposition would lead to the generation of DRs and this was only observed for the super composite transposon carrying the *libA* locus. A first step in such a transposition event, would lead to a cointegrate structure between the original replicon carrying the transposon and the receiving replicon. Interestingly, the cargo of plasmid pPBSH4-2 contains in addition to its two catabolic clusters encoding *ccd* and *hlyA*, genes involved in plasmid replication/stability. The latter might belong to a plasmid that initially carried the transposons and hence be remnants of such a cointegrate structure. Another mode of transposition of *IS1071* associated (catabolic) genes might involve the recent described concept of translocatable unit (TU) as recently shown for the mobility of antibiotic resistance genes associated with *IS26*. TUs consist of a unique DNA segment containing genes and a single copy of an IS element. The TU structure performs RecA-independent incorporation next to a second IS identical to the IS carried by the TU, resulting into structures resembling composite transposons with the two IS in direct orientation (Harmer et al. 2014; Hudson et al. 2014; He et al. 2015). Repeating this process would result into the arrays of catabolic genes we have observed with directly oriented copies of *IS1071* at each end and between each unique segment. The involvement of TUs in IS associated mobility of cargo genes has however only been reported for ISs belonging to the *IS6* family (like *IS26*) and not for ISs of the *Tn3* family (like *IS1071*). Another explanation of the observed multimeric composite transposon array configuration with shared *IS1071* elements between two adjoining composite transposons might be linked with homologous recombination between two outer *IS1071* elements of two nearby newly acquired discrete composite transposons. Whatever the process of transposition of the *IS1071* associated catabolic gene clusters might be, as discussed above, the strong conservative nature of the catabolic loci suggests that the recruitment of the different catabolic clusters in the linuron-degrading *Variovorax* strains is rather due to the recruitment of already existing catabolic composite transposon structures than by the assembly process itself.

Next to *IS1071*, plasmids appear to play an essential role in the genetic adaptation of *Variovorax* toward linuron catabolism. Broad host range plasmids such as IncP-1 are known to distribute catabolic clusters in communities and catabolic IncP-1 plasmids often contain *IS1071* associated catabolic composite transposons (Boon et al. 2001; Król et al. 2012). Interestingly, each of the linuron degraders with the exception of WDL1 carries at least one plasmid of a well-known promiscuous plasmid group (IncP-1 or PromA). Their involvement in distributing linuron catabolic genes in the linuron-degrading strains is suggested from the fact that these plasmids all carry at least one of the linuron catabolic gene functions with the exception of pPBL-H6-2. However, the latter carries an *IS1071* copy and hence, as mentioned above might have been involved in initial recruitment of the composite transposon

carrying the linuron catabolic locus in PBL-H6-2. After transposition of the composite transposon carrying the catabolic genes onto pPBL-H6-1, deletion of the catabolic genes might have taken place due to recombination between the *IS1071* ISs flanking the catabolic locus. Such an event was reported before for a similar composite transposon structure carrying atrazine catabolic genes (Devers et al. 2007). In addition, other plasmids of yet unknown type, carrying signs of conjugative features, were present. Likely, plasmids move around in a community, and pick up the composite transposons either by transposition as a discrete unit or by involving TU, for further transfer to their final hosts. As such, the BHR plasmids found in the linuron-degrading strains might have, next to *IS1071*, functioned as a second crucial vehicle for acquisition of the catabolic genes.

Regarding catabolic functions, only a limited reservoir of catabolic loci was utilized for integration in the linuron catabolic pathways indicating that the source of suitable catabolic functions for composing a functional linuron catabolic pathway in *Variovorax* is limited, even on a worldwide scale. Curiously, these genes seem only to be recruited by a specific clade 1 of *Variovorax*, whose members, in addition to linuron, seem to be prone to genetic adaptation and hence specialization toward the biodegradation of other anthropogenic compounds. Apparently, for unknown reasons, this clade is able to recruit and express foreign genes for xenobiotic biodegradation. Sequence analysis of other genomes within this clade, in addition to the linuron degraders, and comparison with the genome sequences of clade 2, might unravel the mechanisms involved in this special ability of catabolic gene recruitment.

## Supplementary Material

Supplementary data are available at *Genome Biology and Evolution* online.

## Acknowledgments

We thank Sebastian S. Sørensen and Koji Satsuma for the donation of strains SRS16 and RA8, Simone Severitt for technical assistance, Markus Göker, Jörn Petersen, Kornelia Smalla, Masa Shintani, and Isabel Schober for valuable discussions regarding the article, and Jörg Overmann for his support with the sequencing of the strains. We acknowledge funding by Fonds voor Wetenschappelijk Onderzoek – Vlaanderen (FWO) Project G.0371.06, and the EU project METAEXPLORE (EU Grant No. 222625). J.M.K. was supported by Deutsche Forschungsgemeinschaft within “Sonderforschungsbereich TRR 51.” We acknowledge the use of de.NBI cloud and the support by the High Performance and Cloud Computing Group at the Zentrum für Datenverarbeitung of the University of Tübingen, the Federal Ministry of Education and Research (BMBF) (Grant

Number 031 A535A). The open access publication of this study was funded by the Leibniz Open Access Publishing Fund (Grant No. 4055).

## Literature Cited

- Alamos P, et al. 2018. Functionality of tRNAs encoded in a mobile genetic element from an acidophilic bacterium. *RNA Biol.* 15(4–5):518–527.
- Albers P, Lood C, et al. 2018. Catabolic task division between two near-isogenic subpopulations co-existing in a herbicide-degrading bacterial consortium: consequences for the interspecies consortium metabolic model. *Environ Microbiol.* 20(1):85–96.
- Albers P, Weytjens B, De Mot R, Marchal K, Springael D. 2018. Molecular processes underlying synergistic linuron mineralization in a triple-species bacterial consortium biofilm revealed by differential transcriptomics. *Microbiologyopen* 7(2):e00559–e00614.
- Armalyte J, Jurenaite M, Beinoraviciute G, Teiserskas J, Suziedeliene E. 2012. Characterization of *Escherichia coli* *dinJ-yafQ* toxin-antitoxin system using insights from mutagenesis data. *J Bacteriol.* 194(6):1523–1532.
- Baptista IIR, et al. 2008. Evidence of species succession during chlorobenzene biodegradation. *Biotechnol Bioeng.* 99(1):68–74.
- Barkay T, Miller SM, Summers AO. 2003. Bacterial mercury resistance from atoms to ecosystems. *FEMS Microbiol Rev.* 27(2-3):355–384.
- Bers K, et al. 2011. A novel hydrolase identified by genomic-proteomic analysis of phenylurea herbicide mineralization by *Variovorax* sp. strain SRS16. *Appl Environ Microbiol.* 77(24):8754–8764.
- Bers K, et al. 2013. Hyla, an alternative hydrolase for initiation of catabolism of the phenylurea herbicide linuron in *Variovorax* sp. *Appl Environ Microbiol.* 79(17):5258–5263.
- Boon N, Goris J, De Vos P, Verstraete W, Top EM. 2001. Genetic diversity among 3-chloroaniline- and aniline-degrading strains of the *Comamonadaceae*. *Appl Environ Microbiol.* 67(3):1107–1115.
- Bottacini F, et al. 2015. Discovery of a conjugative megaplasmid in *Bifidobacterium breve*. *Appl Environ Microbiol.* 81(1):166–176.
- Bruegelmans P, D’Huys PJ, De Mot R, Springael D. 2007. Characterization of novel linuron-mineralizing bacterial consortia enriched from long-term linuron-treated agricultural soils. *FEMS Microbiol Ecol.* 64(2):271–282.
- Casacuberta E, González J. 2013. The impact of transposable elements in environmental adaptation. *Mol Ecol.* 22(6):1503–1517.
- Crombie AT, et al. 2018. Poplar phyllosphere harbors disparate isoprene-degrading bacteria. *Proc Natl Acad Sci U S A.* 115(51):13081–13086.
- Cummings MP. 2014. PAUP\* (phylogenetic analysis using parsimony (and other methods)). *Dict Bioinforma Comput Biol.* <https://doi.org/10.1002/9780471650126.dob0522.pub2>
- Dejonghe W, et al. 2003. Synergistic degradation of linuron by a bacterial consortium and isolation of a single linuron-degrading *Variovorax* strain. *Appl Environ Microbiol.* 69(3):1532–1541.
- Devers M, Rouard N, Martin-Laurent F. 2007. Genetic rearrangement of the *atzAB* atrazine-degrading gene cassette from pADP1::Tn5 to the chromosome of *Variovorax* sp. MD1 and MD2. *Gene* 392(1–2):1–6.
- Di Gioia D, Peel M, Fava F, Wyndham RC. 1998. Structures of homologous composite transposons carrying *cbaABC* genes from Europe and North America. *Appl Environ Microbiol.* 64(5):1940–1946.
- Dunon V, Bers K, Lavigne R, Top EM, Springael D. 2018. Targeted metagenomics demonstrates the ecological role of IS1071 in bacterial community adaptation to pesticide degradation. *Environ Microbiol.* 20(11):4091–4111.
- Dunon V, et al. 2013. High prevalence of IncP-1 plasmids and IS1071 insertion sequences in on-farm biopurification systems and other pesticide-polluted environments. *FEMS Microbiol Ecol.* 86(3):415–431.
- Franke S, Grass G, Rensing C, Nies DH. 2003. Molecular analysis of the copper-transporting efflux system CusCFBA of *Escherichia coli*. *J Bacteriol.* 185(13):3804–3812.
- Fulthorpe RR, Wyndham RC. 1992. Involvement of a chlorobenzoate-catabolic transposon, Tn5271, in community adaptation to chlorobiphenyl, chloroaniline, and 2,4-dichlorophenoxyacetic acid in a freshwater ecosystem. *Appl Environ Microbiol.* 58(1):314–325.
- Garcillán-Barcia MP, Francia MV, de La Cruz F. 2009. The diversity of conjugative relaxases and its application in plasmid classification. *FEMS Microbiol Rev.* 33(3):657–687.
- Garcillán-Barcia MP, Redondo-Salvo S, Vielva L, de la Cruz F. 2020. MOBscan: automated annotation of MOB relaxases. *Methods Mol Biol.* 2075:295–308.
- Godde JS, Bickerton A. 2006. The repetitive DNA elements called CRISPRs and their associated genes: evidence of horizontal transfer among prokaryotes. *J Mol Evol.* 62(6):718–729.
- Harmer CJ, Moran RA, Hall RM. 2014. Movement of IS26-associated antibiotic resistance genes occurs via a translocatable unit that includes a single IS26 and preferentially inserts adjacent to another IS26. *MBio* 5(5):e01801–e01814.
- Harrison PW, Lower RPJ, Kim NKD, Young J. 2010. Introducing the bacterial ‘chromid’: not a chromosome, not a plasmid. *Trends Microbiol.* 18(4):141–148.
- He S, et al. 2015. Insertion sequence IS26 reorganizes plasmids in clinically isolated multidrug-resistant bacteria by replicative transposition. *MBio* 6(3):e00762–e00815.
- Hudson CM, Bent ZW, Meagher RJ, Williams KP. 2014. Resistance determinants and mobile genetic elements of an NDM-1-encoding *Klebsiella pneumoniae* strain. *PLoS One* 9(6):e99209.
- Jiang W, Metcalf WW, Lee KS, Wanner BL. 1995. Molecular cloning, mapping, and regulation of Pho regulon genes for phosphonate breakdown by the phosphonatase pathway of *Salmonella typhimurium* LT2. *J Bacteriol.* 177(22):6411–6421.
- Kim DU, Kim MS, Lim JS, Ka JO. 2013. Widespread occurrence of the *tfd-II* genes in soil bacteria revealed by nucleotide sequence analysis of 2,4-dichlorophenoxyacetic acid degradative plasmids pDB1 and p712. *Plasmid* 69(3):243–248.
- Kim DW, Lee K, Lee DH, Cha CJ. 2018. Comparative genomic analysis of pyrene-degrading *Mycobacterium* species: genomic islands and ring-hydroxylating dioxygenases involved in pyrene degradation. *J Microbiol.* 56(11):798–804.
- Koonin EV, Makarova KS, Zhang F. 2017. Diversity, classification and evolution of CRISPR-Cas systems. *Curr Opin Microbiol.* 37:67–78.
- Król JE, et al. 2012. Role of IncP-1β plasmids pWDL7::rfp and pNB8c in chloroaniline catabolism as determined by genomic and functional analyses. *Appl Environ Microbiol.* 78(3):828–838.
- Le S, Josse J, Ois Husson F. 2008. FactoMineR: an R package for multivariate analysis. *J Stat Software Artic.* 25:1–18.
- Lechner M, et al. 2011. Proteinortho: detection of (co-)orthologs in large-scale analysis. *BMC Bioinformatics* 12(1):124.
- Lefort V, Desper R, Gascuel O. 2015. FastME 2.0: a comprehensive, accurate, and fast distance-based phylogeny inference program. *Mol Biol Evol.* 32(10):2798–2800.
- Legatzki A, Grass G, Anton A, Rensing C, Nies DH. 2003. Interplay of the Czc system and two P-type ATPases in conferring metal resistance to *Ralstonia metallidurans*. *J Bacteriol.* 185(15):4354–4361.
- Letunic I, Bork P. 2019. Interactive Tree Of Life (iTOL) v4: recent updates and new developments. *Nucleic Acids Res.* 47(W1):W256–W259.
- Li H, Durbin R. 2009. Fast and accurate short read alignment with Burrows-Wheeler transform. *Bioinformatics* 25(14):1754–1760.

- Li X, et al. 2018. oriTFinder: a web-based tool for the identification of origin of transfers in DNA sequences of bacterial mobile genetic elements. *Nucleic Acids Res.* 46(W1):W229–W234.
- Liang Q, et al. 2005. Chromosome-encoded gene cluster for the metabolic pathway that converts aniline to TCA-cycle intermediates in *Delftia tsuruhatensis* AD9. *Microbiology* 151(10):3435–3446.
- Mahan KM, et al. 2017. Iron-dependent enzyme catalyzes the initial step in biodegradation of N-nitrotyrosine by *Variovorax* sp. strain JS1663. *Appl Environ Microbiol.* 83:1–10.
- Martinez B, Tomkins J, Wackett LP, Wing R, Sadowsky MJ. 2001. Complete nucleotide sequence and organization of the atrazine catabolic plasmid pADP-1 from *Pseudomonas* sp. strain ADP. *J Bacteriol.* 183(19):5684–5697.
- Meier-Kolthoff JP, Auch AF, Klenk H-P, Göker M. 2013. Genome sequence-based species delimitation with confidence intervals and improved distance functions. *BMC Bioinformatics* 14(1):60.
- Meier-Kolthoff JP, Auch AF, Klenk H, Göker M. 2014. Highly parallelized inference of large genome-based phylogenies. *Concurrency Comput Pract Exp.* 26(10):1715–1729.
- Meier-Kolthoff JP, Göker M. 2017. VICTOR: genome-based phylogeny and classification of prokaryotic viruses. *Bioinformatics* 33(21):3396–3404.
- Meier-Kolthoff JP, Göker M. 2019. TYGS is an automated high-throughput platform for state-of-the-art genome-based taxonomy. *Nat Commun.* 10(1):2182.
- Mela F, et al. 2008. Comparative genomics of the pIPO2/pSB102 family of environmental plasmids: sequence, evolution, and ecology of pTer331 isolated from *Collimonas fungivorans* Ter331. *FEMS Microbiol. Ecol.* 66(1):45–62.
- Morgado SM, Vicente A. 2018. Beyond the limits: tRNA array units in *Mycobacterium* genomes. *Front Microbiol.* 9:1042. <https://www.frontiersin.org/article/10.3389/fmicb.2018.01042>.
- Nakatsu C, Ng J, Singh R, Straus N, Wyndham C. 1991. Chlorobenzoate catabolic transposon Tn5271 is a composite class-I element with flanking class-II insertion sequences. *Proc Natl Acad Sci U S A.* 88(19):8312–8316.
- Parks D. 2017. CompareM. Available from: <https://github.com/dparks1134/CompareM>. Accessed April 30, 2020.
- Pattengale ND, Alipour M, Bininda-Emonds ORP, Moret BME, Stamatakis A. 2010. How many bootstrap replicates are necessary? *J Comput Biol.* 17(3):337–354.
- Plumeier I, Pérez-Pantoja D, Heim S, González B, Pieper DH. 2002. Importance of different *tfd* genes for degradation of chloroaromatics by *Ralstonia eutropha* JMP134. *J Bacteriol.* 184(15):4054–4064.
- Pope WH, et al. 2014. Cluster M mycobacteriophages Bongo, PegLeg, and Rey with unusually large repertoires of tRNA isotypes. *J Virol.* 88(5):2461–2480.
- Pothier JF, et al. 2011. The ubiquitous plasmid pXap41 in the invasive phytopathogen *Xanthomonas arboricola* pv. *pruni*: complete sequence and comparative genomic analysis. *FEMS Microbiol Lett.* 323(1):52–60.
- Providenti MA, et al. 2006. The locus coding for the 3-nitrobenzoate dioxygenase of *Comamonas* sp. strain JS46 is flanked by IS1071 elements and is subject to deletion and inversion events. *Appl Environ Microbiol.* 72(4):2651–2660.
- Pruesse E, Peplies J, Glöckner FO. 2012. SINA: accurate high-throughput multiple sequence alignment of ribosomal RNA genes. *Bioinformatics* 28(14):1823–1829.
- Puerto-Galan L, Vioque A. 2012. Expression and processing of an unusual tRNA gene cluster in the cyanobacterium *Anabaena* sp. PCC 7120. *FEMS Microbiol Lett.* 337(1):10–17.
- Quast C, et al. 2012. The SILVA ribosomal RNA gene database project: improved data processing and web-based tools. *Nucleic Acids Res.* 41(D1):D590–D596.
- Rensing C, Pribyl T, Nies DH. 1997. New functions for the three subunits of the CzcCBA cation-proton antiporter. *J Bacteriol.* 179(22):6871–6879.
- Sakai Y, Ogawa N, Shimomura Y, Fujii T. 2014. A 2, 4-dichlorophenoxy-acetic acid degradation plasmid pM7012 discloses distribution of an unclassified megaplasmid group across bacterial species. *Microbiology* 160(3):525–536.
- Sasoh M, et al. 2006. Characterization of the terephthalate degradation genes of *Comamonas* sp. strain E6. *Appl Environ Microbiol.* 72(3):1825–1832.
- Satola B, Wübbeler JH, Steinbüchel A. 2013. Metabolic characteristics of the species *Variovorax paradoxus*. *Appl Microbiol Biotechnol.* 97(2):541–560.
- Satsuma K. 2010. Mineralisation of the herbicide linuron by *Variovorax* sp. strain RA8 isolated from Japanese river sediment using an ecosystem model (microcosm). *Pest Manag Sci.* 66(8):847–852.
- Seemann T. 2014. Prokka: rapid prokaryotic genome annotation. *Bioinformatics* 30(14):2068–2069.
- Sen D, et al. 2010. Comparative genomics of pAKD4, the prototype IncP-1 $\delta$  plasmid with a complete backbone. *Plasmid* 63(2):98–107.
- Serfiotis-Mitsa D, et al. 2010. The structure of the KlcA and ArdB proteins reveals a novel fold and antirestriction activity against Type I DNA restriction systems in vivo but not in vitro. *Nucleic Acids Res.* 38(5):1723–1737.
- Shingler V, Powlowski J, Marklund U. 1992. Nucleotide sequence and functional analysis of the complete phenol/3,4-dimethylphenol catabolic pathway of *Pseudomonas* sp. strain CF600. *J Bacteriol.* 174(3):711–724.
- Smillie C, Garcillán-Barcia MP, Francia MV, Rocha EPC, de la Cruz F. 2010. Mobility of plasmids. *Microbiol Mol Biol Rev.* 74(3):434–452.
- Sørensen SR, et al. 2005. Elucidating the key member of a linuron-mineralizing bacterial community by PCR and reverse transcription-PCR denaturing gradient gel electrophoresis 16S rRNA gene fingerprinting and cultivation. *Appl Environ Microbiol.* 71(7):4144–4148.
- Sota M, Kawasaki H, Tsuda M. 2003. Structure of haloacetate-catabolic IncP-1beta plasmid pUO1 and genetic mobility of its residing haloacetate-catabolic transposon. *J Bacteriol.* 185(22):6741–6745.
- Stamatakis A. 2014. RAxML version 8: a tool for phylogenetic analysis and post-analysis of large phylogenies. *Bioinformatics* 30(9):1312–1313.
- Tabata M, et al. 2016. Comparison of the complete genome sequences of four  $\gamma$ -hexachlorocyclohexane-degrading bacterial strains: insights into the evolution of bacteria able to degrade a recalcitrant man-made pesticide. *DNA Res.* 23(6):581–599.
- Tsai KJ, Yoon KP, Lynn AR. 1992. ATP-dependent cadmium transport by the *cadA* cadmium resistance determinant in everted membrane vesicles of *Bacillus subtilis*. *J Bacteriol.* 174(1):116–121.
- Van der Auwera GA, et al. 2009. Plasmids captured in *C. metallidurans* CH34: defining the PromA family of broad-host-range plasmids. *Antonie Van Leeuwenhoek.* 96(2):193–204.
- Veltri D, Wight MM, Crouch JA. 2016. SimpleSynteny: a web-based tool for visualization of microsynteny across multiple species. *Nucleic Acids Res.* 44(W1):W41–W45.
- Wang Y, et al. 2017. Quantifying the importance of the rare biosphere for microbial community response to organic pollutants in a freshwater ecosystem. *Appl Environ Microbiol.* 83:1–19.
- Werner J, et al. 2020. PromA plasmids are instrumental in the dissemination of linuron catabolic genes between different genera. *Front Microbiol.* 11:149.
- Woo HL, et al. 2017. High-quality draft genome sequences of four lignocellulose-degrading bacteria isolated from Puerto Rican forest

- soil: *Gordonia* sp., *Paenibacillus* sp., *Variovorax* sp., and *Vogesella* sp. *Genome Announc.* 5(18):e00300–17.
- Xia XS, Aathithan S, Oswiecimska K, Smith ARW, Bruce IJ. 1998. A novel plasmid pJJB1 possessing a putative 2,4-dichlorophenoxyacetate degradative transposon Tn5530 in *Burkholderia cepacia* strain 2a. *Plasmid* 39(2):154–159.
- Yanagiya K, et al. 2018. Novel self-transmissible and broad-host-range plasmids exogenously captured from anaerobic granules or cow manure. *Front Microbiol.* 9:1–12.
- Zhang HJ, et al. 2012. Biotransformation of the neonicotinoid insecticide thiacloprid by the bacterium *Variovorax boronicumulans* strain J1 and mediation of the major metabolic pathway by nitrile hydratase. *J Agric Food Chem.* 60(1):153–159.
- Zhang M, Brons JK, van Elsas JD. 2016. The complete sequences and ecological roles of two IncP-1 $\beta$  plasmids, pHB44 and pBS64, isolated from the mycosphere of *Laccaria proxima*. *Front Microbiol.* 7:1–11.
- Zhang M, et al. 2015. IncP-1 $\beta$  plasmids are important carriers of fitness traits for *Variovorax* species in the mycosphere—two novel plasmids, pHB44 and pBS64, with differential effects unveiled. *Microb Ecol.* 70(1):141–153.

Associate editor: Laura A. Katz